The Impact of Kinetically Restricted Structure on Thermal Conversion of Zinc Tetraphenylporphyrin Thin Films to the Triclinic and Monoclinic Phases

Nobutaka Shioya,[†] Miyako Hada,[†] Takafumi Shimoaka,[†] Richard Murdey,[‡] Kazuo Eda,[§] and Takeshi Hasegawa*[,†]

[†] Laboratory of Chemistry for Functionalized Surfaces, Division of Environmental Chemistry, Institute for Chemical Research, Kyoto University, Gokasho, Uji, Kyoto 611-0011, Japan

[‡] Laboratory of Molecular Aggregation Analysis, Division of Multidiscipinary Chemistry, Institute for Chemical Research, Kyoto University, Gokasho, Uji, Kyoto 611-0011, Japan

[§] Department of Chemistry, Graduate School of Science, Kobe University, 1-1 Rokko-dai, Nada-ku, Kobe, Hyogo 657-8501, Japan

[†] To whom correspondence should be addressed.

E-mail: htakeshi@scl.kyoto-u.ac.jp

ABSTRACT: The powerful combination of p-polarized multiple-angle incidence resolution spectroscopy (pMAIRS) and grazing incidence X-ray diffraction (GIXD) is applied to the structural characterization of zinc tetraphenylporphyrin (ZnTPP) in vapor-deposited films as a function of the deposition rate. The deposition rate is revealed to have an impact on the initial film structure and its conversion by thermal annealing. The pMAIRS spectra reveal that a fast deposition rate yields a kinetically restricted amorphous film of ZnTPP having a 'face-on orientation,' which is readily discriminated from another 'randomly oriented' amorphous film generated at a slow deposition rate. In addition, the GIXD patterns reveal that the film grown at a slow deposition rate involves a minor component of triclinic crystallites. The different initial film structure significantly influences the thermal conversion of ZnTPP films. The randomly oriented amorphous aggregates with the triclinic crystallite-seeds are converted to the thermodynamically stable phase (monoclinic) via the metastable triclinic phase. The kinetically restricted structure, on the other hand, is followed by a simple thermal conversion: the molecules are directly converted to the monoclinic one rather than the triclinic one.

INTRODUCTION

Porphyrin has a functionalizable skeleton and its derivatives are employed to make an active layer in organic thin film devices.[1-14] Zinc tetraphenylporphyrin (ZnTPP; Figure 1) is a solvent-soluble low molecular-weight material, and a thin film can be prepared by both dry- and wet-processes. The spin-coated thin film is, for example, used as a p-type semiconductor in organic photovoltaic devices,[7,8] while the vapor-deposited film is incorporated in gas sensors.[9] Comprehensive understanding of the structure-controlling factors for both wet- and dry-films is thus of great importance, since the device properties are closely correlated with the film structure.[6] Unfortunately, however, the structural analysis of the ZnTPP thin film is very limited,[15-18] although many studies have been reported on the device applications.[6-14]

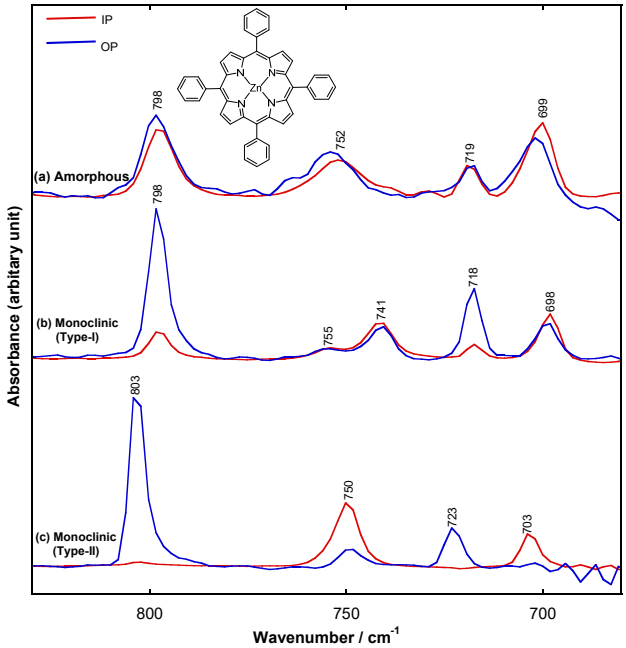

Figure 1 The correlation between the polymorphs and the γ(C–H) band for the ZnTPP casted films:[25] the spin-coated film prepared from a chloroform solution exhibits amorphous (a), and the thermally-annealed film belongs to the monoclinic crystal (Type-I) of ZnTPP (b). When a low-volatile solvent of 1,2,4-trichlorobenzene (TCB) is used, another monoclinic phase (Type-II) is formed in the film (c).

Thin films of organic semiconductors such as porphyrin and phthalocyanine are generally not suitable for an X-ray diffraction (XRD) analysis due to the low diffraction intensity in the thin film. An as-grown film, in fact, is known to give almost no diffraction signals,[6,16,19,20] which results in a misleading impression that all these films are composed of the randomly oriented amorphous portions, since the XRD pattern retrieves no orientation information for minute fractions of both crystallites and amorphous aggregates.

In recent years, keen attention is attracted for p-polarized multiple-angle incidence resolution spectrometry (pMAIRS)[21-23] as a powerful tool for characterizing the polymorphs and molecular orientation in such a low-crystallinity film. For the pMAIRS analysis, the C–H out-of-plane deformation vibration (denoted as γ(C–H)) band of an aromatic ring is a highly useful band for discussing the molecular structure in an organic semiconductor thin film, since the band intensity and position are correlated with the ring orientation and the polymorphs, respectively.[24-27] As noted in Figure 1, some representative polymorphs of ZnTPP have already been revealed to have specific pMAIRS spectra having different patterns.[25] In fact, once the correlation between the pMAIRS and grazing incidence X-ray diffraction (GIXD) data is obtained, the molecular structure in terms of the molecular orientation and the polymorphs in a ZnTPP casted film can be revealed by the pMAIRS spectra alone.[25]

In the present study, the powerful combination technique of pMAIRS and GIXD is first employed for the structural analysis of ZnTPP in a 'vapor-deposited' thin film. In our former study, the dominant factor for controlling the molecular structure in a 'casted film' was revealed to be the 'evaporation time' of solvent. In other words, the "film-forming time" is the key factor, which gives us an impression that 'vapor-deposited films' should also be controlled by changing the deposition rate of the vacuum evaporation. As

the deposition rate increases, in general, the rate of nucleation increases, which yields a kinetically stable or restricted structure.[28,29] Actually, previous reports demonstrate that the deposition rate has a substantial impact on the resulting crystal phase and its crystallinity of some organic semiconductors in evaporated films.[29-31] Therefore, the present study focuses on the effect of deposition rate on the initial film structure of ZnTPP, followed by a structural conversion by thermal annealing. The deposition rate is found to significantly influence not only the initial structure, but also the thermal conversion of the film via two different intermediate amorphous states.

EXPERIMENTAL METHODS

Film Preparation: Zinc(II) tetraphenylporphyrin (ZnTPP) was provided by Tokyo Chemical Industry Co. Ltd. (Tokyo, Japan), which was used without further purification. The Si wafer having a thickness of 0.675 ± 0.025 mm was purchased from Valqua FFT (Tokyo, Japan), and it was chemically treated to have a hydrophobic surface by using a octadecyltrimethoxysilane (ODS) solution (0.5%) of an organic solvent involving methylethylbenzene (SAMLAY®-A)[32,33] that was provided by courtesy of Nippon Soda Co., Ltd. (Tokyo, Japan). The surface generally has a weak interaction with organic semiconductor molecules, and thus it can be regarded as an inert surface.[34] The vapor-

deposited thin film with a thickness of 50 nm was prepared under a base pressure of 10^{-4} Pa. The sample temperature was maintained at ambient temperature, and the average deposition rate was 80 and 0.2 nm min^{-1} followed by thermal annealing at 100 and 200°C for 2h on a laboratory bench, which are named fast- and slow-deposition, respectively. The fast- and slow-deposited thin films of ZnTPP are denoted as the FD-*T* and SD-*T* films (*T*; annealing temperature), respectively, throughout this paper.

Film Characterization: The GIXD patterns (with an in-plane geometry) were recorded by a RIGAKU (Tokyo, JAPAN) SuperLab diffractometer at ambient temperature. The X-ray was generated by using a Cu rotating anode X-ray generator at 40 kV and 30 mA (Cu Kα radiation). The incident angle of X-ray was fixed at 0.2° from the surface parallel. The pMAIRS spectra were measured on a Thermo Fischer Scientific (Madison, WI) Nicolet 6700 FT-IR spectrometer equipped with a Thermo Fischer Scientific (Yokohama, Japan) automatic MAIRS equipment (TN 10-1500) under the optimal condition determined for a Si substrate.[23] The p-polarized IR ray was generated through a Harrick Scientific (Pleasantville, NY) PWG-U1R wire-grid polarizer, and it was detected by a MCT detector. The interferogram was measured 500 times for each angle. The experimental details are referred to our former study.[25]

The orientation angle, ϕ, of a transition moment can simply be calculated by

using the dichroic ratio of pMAIRS-IP (in-plane) to -OP (out-of-plane) spectra ($A_{\mathrm{IP}}/A_{\mathrm{OP}}$) as long as the optimized experimental conditions are employed[23,35]:

$$\phi = \tan^{-1}\sqrt{\frac{2A_{\mathrm{IP}}}{A_{\mathrm{OP}}}}\ , \qquad (1)$$

where ϕ is the averaged orientation angle from the surface normal.

RESULTS AND DISCUSSION

Effect of deposition rate on the initial film structure of ZnTPP: Figure 2a presents GIXD-IP patterns of ZnTPP-FD and -SD films without thermal annealing. No apparent diffraction peaks are observed and no significant difference is found between the two patterns, which indicate that the structure of both films is nearly amorphous. In fact, the pMAIRS spectral pattern in the γ(C–H) region of 850-650 cm^{-1} (Figure 2b) also indicates that the films have an amorphous structure: the band positions of the four peaks at 798, 752, 719 and 700 cm^{-1} are all in good agreement with the characteristic bands of the amorphous state as shown in Figure 1a. This result gives us an impression that the deposition rate does not influence an average crystallinity in the film significantly.

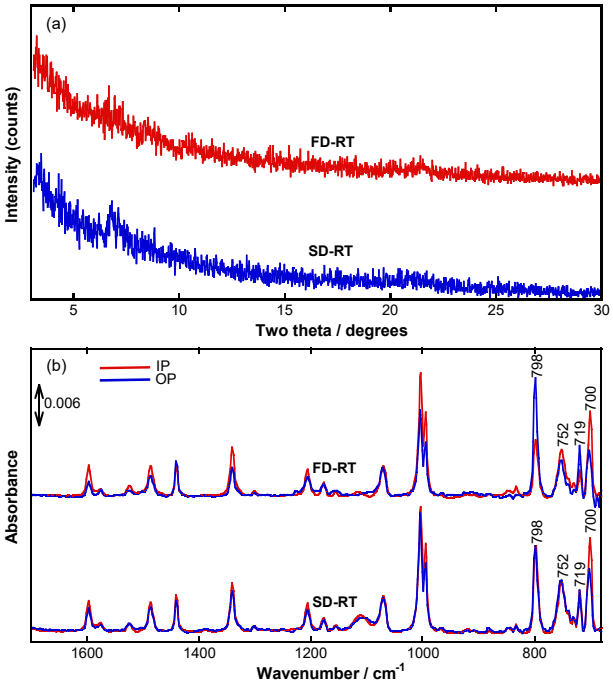

Figure 2　GIXD-IP patterns (a) and pMAIRS spectra (b) of the fast- and slow-deposited films of ZnTPP prepared at ambient temperature.

A large difference is found, however, in the molecular orientation as revealed by the pMAIRS spectra (Figure 2b). The orientation is typically revealed by using the γ(C–H) bands of the aromatic rings of ZnTPP, which are truly useful for discussing the orientation of the porphyrin and the phenyl rings individually. According to the surface selection rule of pMAIRS,[21,22] when the γ(C–H) band appears stronger in the IP spectrum than that in OP one, the rings have the edge-on orientation; whereas the face-on orientation is revealed when the OP band is stronger than the IP one.[25] On this rule, the porphyrin ring in the 'FD' film is found to have the face-on orientation, since the γ(C–H) band appears at 798 cm^{-1} dominantly in the OP spectrum (Figure 2b). The 'SE' film has

a ratio of unity, on the other hand, which holds for most of the bands. This quantitative agreement between the IP and OP spectra means that the molecule involving the porphyrin ring is randomly oriented in the film.

Since the film structure is amorphous, the face-on orientation found in the FD-RT film is not induced by the crystallization of ZnTPP. On considering the fact that the face-on orientation is found only in the "FD" film, the orientation should be a kinetically generated temporal orientation specifically induced by the very fast deposition rate. If this speculation is true, the temporal face-on oriented structure should be relaxed to a randomly oriented structure, followed by crystallization by thermal annealing (or aging).[36] To confirm this expectation, the annealed film is investigated in the next section.

Effect of thermal annealing on the film structure in FD films: Figure 3a presents pMAIRS spectra of the FD films annealed at 100 and 200°C as well as the un-annealed film. When the film is annealed at 100°C (FD-100), most of the IP bands exhibit comparable intensities to the OP ones except a few bands such as the γ(C–H) band at 797 cm^{-1}. Therefore, the molecules become a mostly random orientation (or slightly edge-on orientation) as expected, which implies a structural relaxation. Through this annealing experiment, the face-on orientation in the FD-RT film is thus found to be a kinetically induced frozen structure.

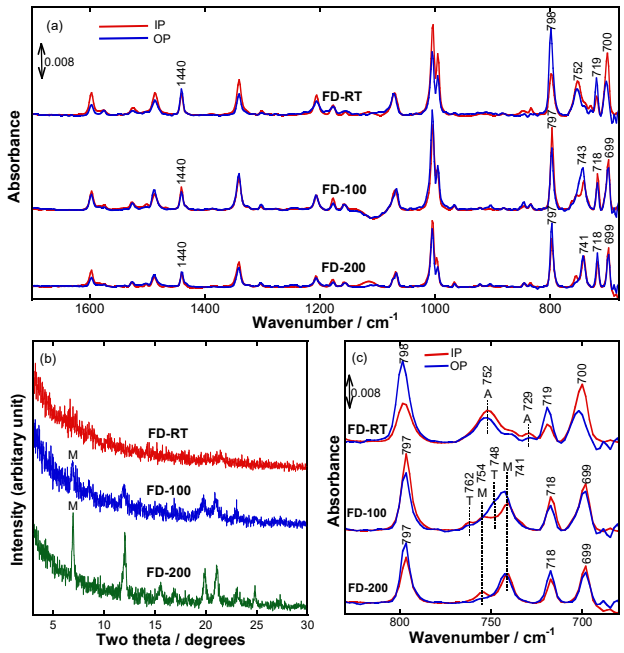

Figure 3 pMAIRS spectra (a) and GIXD-IP patterns (b) of the fast-deposited thin films of ZnTPP. Magnified spectra of the γ(C–H) wavenumber region are shown in (c). The characteristic peaks of the amorphous, monoclinic, and triclinic phases are marked by "A," "M," and "T," respectively.

When the low-wavenumber region is magnified (Figure 3c), the γ(C–H) bands specific to the monoclinic phase are found at 754 and 741 cm^{-1} (marked by "M") particularly in the IP spectrum implying some monoclinic[37] crystallites in the film, whose crystal structure is the same as that of a wet film prepared from a chloroform solution (Figure 1b).[25] This result is supported by the weak XRD peak at 6.9° (Figure 3b) that corresponds to the monoclinic phase.[25,37]

Of note is that another polymorph is also observed with a minor quantity in the FD-100 film by new band components at 762 and 748 cm^{-1} in the pMAIRS spectra (Figure

3c), which are attributed to the triclinic phase[38] of ZnTPP as discussed later. Here, the γ(C–H) band of the 'phenyl' ring at 748 cm^{-1} appears mainly in the OP spectrum, which means that the 'phenyl' rings in the triclinic crystallites have the face-on orientation judging from the surface selection rule of pMAIRS. This further implies that the 'porphyrin' ring is oriented in an edge-on manner, since the porphyrin ring is known to take a nearly perpendicular stance to the phenyl plane in the triclinic crystallites.[38] The triclinic crystallite, regardless, is considered to be minute fragments in the film because no diffraction peak of triclinic is observed in the XRD pattern (Figure 3b). In short, the FD-100 film is concluded to be composed of the randomly oriented monoclinic crystallites (accompanying amorphous aggregates) with major quantity, and minute fragments of the oriented triclinic crystallites.

When the same film is heated up to 200ºC (FD-200), to our surprise, the porphyrin in the FD-200 film gets back to the face-on type like the FD-RT film judging from the γ(C–H) band at 797 cm^{-1} (Figure 3c). This revived face-on orientation should be a result through a different mechanism from that for generating the FD-RT film when referred to the XRD patterns in Figure 3b. Since the diffraction peaks due to the monoclinic phase are clearly observed (Figure 3b), the face-on orientation should have a strong correlation with generation of the monoclinic crystallites of ZnTPP.

Effect of thermal annealing on the film structure in SD films: On the other hand, the SD film has a simple correlation of the molecular orientation with the annealing temperature: the dichroic ratio of the OP band to the IP one increases as the annealing temperature increases, which is typically found for the band at 798 cm^{-1} (Figure 4a). The change of the dichroic ratio indicates that the face-on oriented component increases with increasing the annealing temperature. As noted in the previous section, this orientation is found to be a good correlation with the monoclinic crystallites as found from the XRD pattern (Figure 4b). The SD-200 film, in fact, has the orientation angle of ca. 30° (see Table 1) that is in good agreement with the value[25] of the wet film consisting only of monoclinic crystallites. In other words, the SD-200 film can be recognized to be identical to the spin-coated film (Figure 1b) prepared from the chloroform solution.

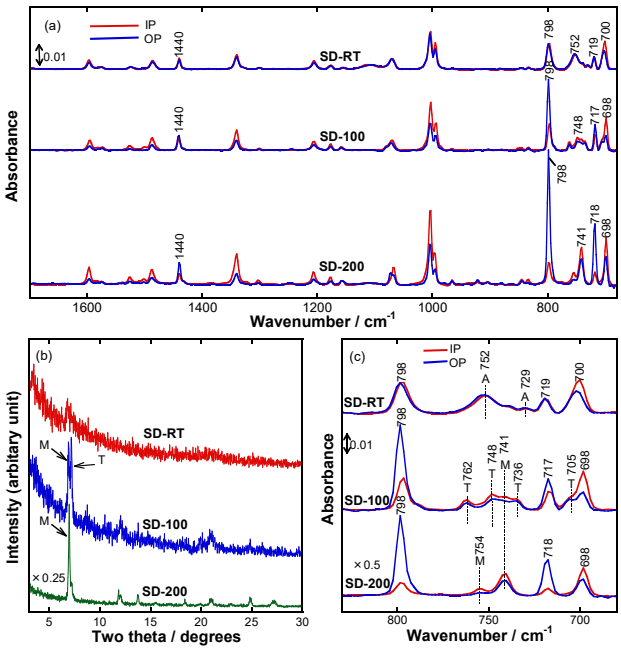

Figure 4 pMAIRS spectra (a) and GIXD-IP patterns (b) of the slow-deposited thin films of ZnTPP. Magnified spectra of the γ(C–H) wavenumber region are shown in (c). The characteristic peaks of the amorphous, monoclinic, and triclinic phases are marked by "A," "M," and "T," respectively.

Table 1 The orientation angle of the porphyrin calculated using the γ(C–H) band at 798 cm^{-1} in the pMAIRS spectra.

Abbreviation	Porphyrin	
	ϕ_{por} / °	Orientation type
FD-RT	44	Face-on
FD-100	59	Random (Slightly edge-on)
FD-200	49	Random (Slightly face-on)
SD-RT	55	Random
SD-100	41	Face-on
SD-200	29	Face-on

The SD-100 film, on the other hand, has a more complicated structure. The XRD pattern (Figure 4b) includes not only the monoclinic peak ($2\theta = 6.9°$)[37], but also the triclinic peak (7.2°)[38]. In a cooperative manner, the pMAIRS spectral pattern is largely different from the SD-200 film (Figure 4c). By comparing the pMAIRS spectra (Figure 4c) with the XRD pattern (Figure 4b), the new bands at 762, 748, 736 and 705 cm^{-1} are readily assigned to the γ(C–H) band of the triclinic crystallites. It should be noted that this triclinic structure is a metastable phase in the thin film, since the triclinic phase is soon

transformed into the monoclinic one when employing a high-annealing temperature of 200°C as found from the GIXD-IP (Figure 4b) and GIXD-OP[25,39] patterns (Figure S1 in the Supporting Information). When using the relatively low temperature of 100°C, therefore, the two types of crystallites coexist, and the annealing process at a high temperature induces the thermodynamically stable structure, i.e., the monoclinic phase.

Influence of deposition rate on the thermal conversion: When comparing the XRD patterns between the FD and SD films (Figures 3b and 4b, respectively), a large difference is found that the triclinic phase of ZnTPP is available specifically in the 'SD' films (as summarized in Figure 5). This implies that the slow-deposition rate promotes nucleation of the triclinic crystallites. In effect, the GIXD-IP pattern of the as-deposited SD film (SD-RT) indicates an ambiguously weak peak at ca. $2\theta = 7.0°$ (Figure 4b), suggesting that a small fraction of crystallites is available. This result can also be confirmed from the GIXD-OP patterns as found in Figure S2, in which the triclinic peak at $2\theta = 7.2°$ is observed only in the SD-RT film.

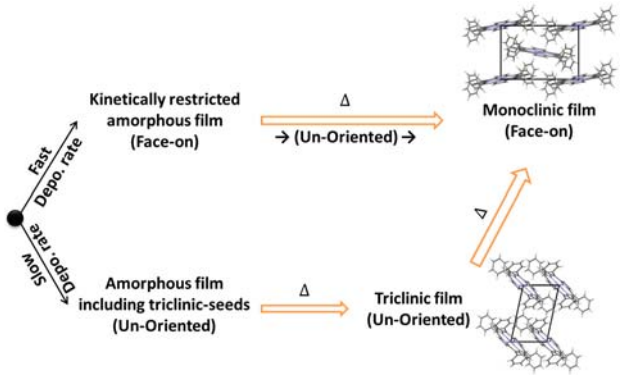

Figure 5 Schematic summary of the different two thermal conversions of ZnTPP thin films grown at fast (80 nm min^{-1}) and slow (0.2 nm min^{-1}) deposition rates.

Difference of the initial film structure influences the following thermal conversion. In the case of SD films, the triclinic crystallite is grown by thermal annealing below 100°C, which yields the clear diffraction peak as well as the monoclinic peak (Figure 4b). By contrast, the FD film annealed at 100°C has the triclinic component alone with an ignorable quantity, and instead a more stable phase, monoclinic, is dominantly formed as discussed above. When annealed at 200°C, both films are composed of the monoclinic phase alone (Figures 3 and 4).

These results indicate that the triclinic phase is obtained by a relatively low molecular dynamics such as a slow deposition and a low temperature annealing. In addition, the triclinic crystallite-seeds generated in the SD-RT film enhance the crystal growth of triclinic with an aid of the thermal annealing. The triclinic phase is thus in a metastable state, which is kinetically favored at room temperature; whereas the

monoclinic phase increases as the temperature increases. The quantity ratio between the monoclinic and triclinic crystallites after the thermal annealing is a function of the number of the triclinic seeds generated in the initial film. In this manner, the balance between the deposition rate and the annealing temperature is the key to produce the metastable triclinic phase.

SUMMARY: Influence of the deposition rate on the thermal conversion of vapor-deposited thin films of ZnTPP has been revealed by using the powerful combination of the pMAIRS and GIXD techniques. The two different amorphous states depending on the deposition rate have readily been found in terms of the molecular orientation by using pMAIRS. A fast deposition rate induces a kinetically restricted face-on orientation, which is discriminated from the random orientation in the SD-RT film. These different amorphous structures yield different thermal conversions. The amorphous aggregates having a random orientation are readily crystallized with improving the orientation with an aid of the thermal annealing. On the other hand, the amorphous components having the face-on orientation found in the kinetically restricted film are first relaxed to be a random orientation followed by crystallization. The GIXD technique also has revealed some changes of crystal structure. The kinetically trapped amorphous aggregates are

directly converted to the thermodynamically stable phase, i.e., the monoclinic phase; whereas the randomly oriented one are changed to the monoclinic phase through the metastable triclinic phase. In addition, the present study has revealed a general rule for obtaining the triclinic crystallite that has not been found in a casted film thus far.

AUTHOR INFORMATION

Corresponding Author: *E-mail: htakeshi@scl.kyoto-u.ac.jp

Notes: The authors declare no competing financial interest.

Supporting Information

The Supporting Information is available free of charge on the ACS Publications website.

GIXD-OP patterns of ZnTPP thin films.

ACKNOWLEDGMENTS

This work was financially supported by a Grant-in-Aid for Scientific Research (A) (No. 15H02185 (TH)), Grant-in-Aid for Young Scientists (B) (No. 17K14502 (TS)) and Grant-in-Aid for JSPS fellows (No. 16J03487 (NS)) from the Japan Society for the Promotion of Science (JSPS), to which the authors' thanks are due.

REFERENCES:

1. Kesters, J.; Verstappen, P.; Kelchtermans, M.; Lutsen, L.; Vanderzande, D.; Maes, W. Porphyrin Based Bulk Heterojunction Organic Photovoltaics: The Rise of the Colors of Life. *Adv. Energy Meter.* **2015**, *5*, 1500218.

2. Walter, M. G.; Rudine, A. B.; Wamser, C. C. Porphyrins and Phthalocyanines in Solar Photovoltaic Cells. *J. Porphyrins Phthlocyanines* **2010**, *14*, 759–792.

3. Ishihara, S.; Labuta, J.; Rossom, W.; Ishikawa, D.; Minami, K.; Hill, J. P.; Ariga, K. Porphyrin-Based Sensor Nanoarchitectonics in Diverse Physical Detection Modes. *Phys. Chem. Chem. Phys.* **2014**, *16*, 9713–9746.

4. Jin, S.; Hill, J. P.; Ji, Q.; Shrestha, L. K.; Ariga, K. Supercapacitive hybrid materials from the thermolysis of porous coordination nanorods based on a catechol porphyrin. *J. Mater. Chem. A* **2016**, *4*, 5737–5744.

5. Mihara, N.; Yamada, Y.; Tanaka, K. Programmable Arrangement of Heterometal Ions in a Supramolecular Array of Porphyrin and Phthalocyanine. *Bull. Chem. Soc. Jpn.* **2017**, *90*, 427–435.

6. Trinh, C.; Whited, M.; Steiner, A.; Tassone, C.; Toney, M.; Thompson, M. Chemical Annealing of Zinc Tetraphenylporphyrin Films: Effects on Film Morphology and Organic Photovoltaic Performance. *Chem. Mater.* **2012**, *24*, 2583–2591.

7. Khan, S. M.; Kaur, M.; Heflin, J. R.; Sayyad, M. H. Fabrication and Characterization of ZnTPP:PCBM Bulk Heterojunction (BHJ) Solar Cells. *J. Phys. Chem. Solids* **2011**, *72*, 1430–1435.

8. Oku, T.; Noma, T.; Suzuki, A.; Kikuchi, K.; Kikuchi, S. Fabrication and Characterization of Fullerene/Porphyrin Bulk Heterojunction Solar Cells. *J. Phys. Chem. Solids* **2010**, *71*, 551–555.

9. Ma, X.; Sun, J.; Wang, M.; Hu, M.; Li, G.; Chen, H.; Huang, J. Effects of Fluorination in the Ring of Zinc Tetraphenylporphyrin on its Gas-Response to Volatiles at Room Temperature. *Sensor. Actuat. B* **2006**, *114*, 1035–1042.

10. Leray, I.; Verniéres, M. C.; Loucif-Saibi, R.; Bied-charreton, C.; Faure, J. Porphyrins as Probe Molecules in the Detection of Gaseous Pollutants I: Diffussion of Pyridine in Polystyrene Films Containing Zinc-Tetraphenylporphyrin. *Sensor. Actuat. B* **1996**, *37*, 67–74.

11. Spadavecchia, J.; Rella, R.; Siciliano, P.; Manera, M. G.; Alimelli. A.; Paolesse, R.; Natale, D. C.; D'Amico, A. Optochemical Vapour Detection Using Spin Coated Thin Film of ZnTPP. *Sensor. Actuat. B* **2006**, *115*, 12–16.

12. Itoh, E.; Higuchi, Y.; Furuhata, D. Enhancement of the Open-Circuit Voltage and Hole Conduction of Tetraphenyl Porphyrin/C_{60} Multilayered Photovoltaic Device by

the Insertion of Oxide Hole Collection Layers. *Jpn. J. Appl. Phys.* **2011**, *50*, 01BC14.

13. Kim, Y.; Lim, H.; Ha, C. S. Red Hybrid Organic Light-Emitting Device Fabricated with Molecularly Doped Polyimide Thin Film Containing Hole-Transporting Nanoparticles. *Sol. St. Elect.* **2004**, *48*, 633–640.
14. Jafari, M. R.; Bahrami, B. Emission Properties of Porphyrin Compounds in New Polymeric PS:CBP Host *Appl. Phys. A* **2015**, *119*, 1491–1497.
15. Cudia, C. C.; Vilmercati, P.; Larciprete, R.; Cepek, C.; Zampieri, G.; Sangaletti, L.; Pagliara, S.; Verdini, A.; Cossaro, A.; Floreano, L. et al. Electronic Structure and Molecular Orientation of a Zn-Tetra-Phenyl Porphyrin Multilayer on Si(111). *Surf. Sci.* **2006**, *600*, 4013–4017.
16. Zeyada, H. M.; Makhlouf, M. M.; Ali, M. A. Structural, Optical and Dispersion Properties of 5,10,15,20-Tetraphenyl-21H,23H-Porphyrin Zinc Thin Films. *Jap. J. Appl. Phys.* **2016**, *55*, 022601.
17. Kate, S.; Pop, S.; Esser, N.; Rappich, J.; Zhang, X.; Hinrichs, K. Aging−Induced Optical Anisotropy in Thermally Grown Thin ZnTPP Films on Si. *Phys. Status Solidi B* **2013**, *250*, 1791–1794.
18. Narioka, S.; Ishii, H.; Ouchi, Y.; Yokoyama, T.; Ohta, T.; Seki, K. XANES Spectroscopic Studies of Evaporated Porphyrin Films: Molecular Orientation and

Electronic Structure. *J. Phys. Chem.* **1995**, *99*, 1332–1337.

19. Zanfolim, A. A.; Volpati, D.; Olivati, C. A.; Job, A. E.; Constantino, C. J. L. Structural and Electric-Optical Properties of Zinc Phthalocyanine Evaporated Thin Films: Temperature and Thickness Effects. *J. Phys. Chem. C* **2010**, *114*, 12290–12299.
20. Senthilarasu, S.; Hahn, Y. B.; Lee, S.-H. Structural Analysis of Zinc Phthalocyanine (ZnPc) Thin Films: X-ray Diffraction Study. *J. Appl. Phys.* **2007**, *102*, 043512.
21. Hasegawa, T. Advanced Multiple-Angle Incidence Resolution Spectrometry for Thin-Layer Analysis on a Low-Refractive-Index Substrate. *Anal. Chem.* **2007**, *79*, 4385–4389.
22. Hasegawa, T. A Novel Measurement Technique of Pure Out-of-Plane Vibrational Modes in Thin Films on a Nonmetallic Material with No Polarizer. *J. Phys. Chem. B* **2002**, *106*, 4112–4115.
23. Shioya, N.; Norimoto, S.; Izumi, N.; Hada, M.; Shimoaka, T.; Hasegawa, T. Optimal Experimental Condition of IR pMAIRS Calibrated by Using an Optically Isotropic Thin Film Exhibiting the Berreman Effect. *Appl. Spectrosc.* **2017**, *71*, 901-910.
24. Shioya, N.; Shimoaka, T.; Eda, K.; Hasegawa, T. Controlling Mechanism of Molecular Orientation of Poly(3-alkylthiophene) in a Thin Film Revealed by Using pMAIRS. *Macromolecules* **2017**, *50*, 5090–5097.

25. Hada, M.; Shioya, N.; Shimoaka, T.; Eda, K.; Hada, M.; Hasegawa, T. Comprehensive Understanding of Structure-Controlling Factors of a Zinc Tetraphenylporphyrin Thin Film Using pMAIRS and GIXD Techniques. *Chem. Eur. J.* **2016**, *22*, 16539–16546.

26. Westermeier, C.; Cernescu, A.; Amarie, S.; Liewald, C.; Keilmann, F.; Nickel, B. Sub-Micron Phase Coexistence in Small-Molecule Organic Thin Films Revealed by Infrared Nano-Imaging. *Nat. Commun.* **2014**, *5*, 4101(1–6).

27. Sharp, J. H.; Abkowitz, M. J. Dimeric Structure of a Copper Phthalocyanine Polymorph. *Phys. Chem.* **1973**, *77*, 477–481.

28. Zheng, F.; Park, B.-N.; Seo, S.; Evans, P.; Himpsel, F. J. Orientation of pentacene molecules on SiO_2: From a monolayer to the bulk. *J. Chem. Phys.* **2007**, *126*, 154702.

29. Ruiz, R.; Choudhary, D.; Nickel, B.; Toccoli, T.; Chang, K.-C.; Mayer, A.; Clancy, P.; Blakely, J.; Headrick, R.; Iannotta, S. et al. Pentacene Thin Film Growth. *Chem. Mater.* **2004**, *16*, 4497–4508.

30. Moser, A.; Salzmann, I.; Oehzelt, M.; Neuhold, A.; Flesch, H.-G.; Ivanco, J.; Pop, S.; Toader, T.; Zahn, D. R.; Smilgies, D.-M. A Disordered Layered Phase in Thin Films of Sexithiophene. *Chem. Phys. Lett.* **2013**, *574*, 51–55.

31. Wang, T; Zhu, Y; Science, J.-Q. Molecular Orientation Transformation in Initial Growth Stage of Disk-Like Phthalocyanine during Organic Vapor Deposition Process. *Chem. Sci.* **2012**, *3*, 528–536.

32. Norimoto, S.; Morimine, S.; Shimoaka, T.; Hasegawa, T. Analysis of the Surface Coverage of a Self-Assembled Monolayer of Octadecyl Silane on a Si(100) Surface by Infrared External-Reflection Spectroscopy. *Anal. Sci.* **2013**, *29*, 979–984.

33. Iwasa, J.; Kumazawa, K.; Aoyama, K.; Suzuki, H.; Norimoto, S.; Shimoaka, T.; Hasegawa, T. In Situ Observation of a Self-Assembled Monolayer Formation of Octadecyltrimethoxysilane on a Silicon Oxide Surface Using a High-Speed Atomic Force Microscope. *J. Phys. Chem. C* **2016**, *120*, 2807–2813.

34. Käfer, D.; Ruppel, L.; Witte, G. Growth of pentacene on clean and modified gold surfaces. *Phys. Rev. B* **2007**, *75*, 085309.

35. Shioya, N.; Shimoaka, T.; Murdey, R.; Hasegawa, T. Accurate Molecular Orientation Analysis Using Infrared p-Polarized Multiple-Angle Incidence Resolution Spectrometry (pMAIRS) Considering the Refractive Index of the Thin Film Sample. *Appl. Spectrosc.* **2017**, *71*, 1242–1248.

36. Sugimoto, S.; Inutsuka, M.; Kawaguchi, D.; Tanaka, K. Reorientation Kinetics of Local Conformation of Polyisoprene at Substrate Interface. *Acs Macro. Lett.* **2018**, 7, 85–89.

37. Byrn, M.; Curtis, C.; Hsiou, Y.; Khan, S. Porphyrin Sponges: Conservative of Host Structure in over 200 Porphyrin-Based Lattice Clathrates. *J. Am. Chem. Soc.* **1993**, *115*, 9480–9497.

38. Scheidt, R.; Mondal, J.; Eigenbrot, C. W.; Adler, A.; Radonovich, L. J.; Hoard, J. L. Crystal and Molecular Structure of the Silver(II) and Zinc(II) Derivatives of Meso-Tetraphenylporphyrin. An Exploration of Crystal-Packing Effects on Bond Distance. *Inorg. Chem.* **1986**, *25*, 795–799.

39. Omote, K.; Harada, J. Grazing-Incidence X-Ray Diffractometer for Determining In-Plane Structure of Thin Films. *Adv. X-ray Anal.* **2000**, *43*, 192–200.

TOC Graphic

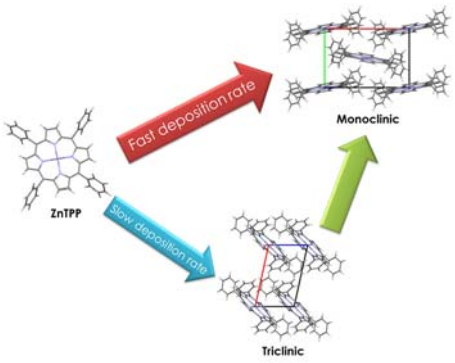
Fast deposition rate
Monoclinic
ZnTPP
Slow deposition rate
Triclinic